XIX IMEKO World Congress
Fundamental and Applied Metrology
September 6–11, 2009, Lisbon, Portugal

WELD TESTING USING EDDY CURRENT PROBES AND IMAGE PROCESSING

Octavian Postolache [1,2], *Artur Lopes Ribeiro*[1], *Helena Ramos*[1]

[1] Instituto de Telecomunicações, Lisboa, Portugal, email: opostolache@lx.it.pt
[2] LabIM, Escola Superior de Tecnologia, Setúbal

Abstract – This paper proposes an eddy-current non-destructive weld testing solution that uses a sensing probe including an excitation coil and a giant magneto-resistance sensor. The testing system control and the acquisition tasks are performed using a PXI system that includes a sinusoidal signal generator, a data acquisition module and a XY scanning stage control interface. For different positions of the sensing probe on the aluminum weld plane the eddy currents are detected and the acquired signals are processed. The signal processing is based on the LabVIEW tone measurement function in order to obtain an image representing the detected voltages as a function of the xy coordinates. An image processing block was designed and implemented in order to detect the weld zone anomalies. This block includes normalization, grayscale image filtering and image segmentation algorithms. Results on weld zone characterization for different tested specimens are included in the paper.

Keywords: – *weld testing, eddy current probes, image processing.*

1. INTRODUCTION

Eddy current testing has the advantage of non-contact and fast test method over other non-destructive testing methods. However, one of the disadvantages of eddy current testing is that it tends to generate large noise due to variations of many factors such as probe lift-off and electromagnetic characteristics of the material under test. For the particular case of welded zone testing the conventional eddy current method [1] performance is strongly affected by shape changes and variable electromagnetic characteristics on the tested regions. In order to overpass these problems several eddy current probe architectures are reported in the literature [2] and are normally based on excitation and detection coil sets [3]. Latest works on flaw and crack detection in conductive plates underline the capabilities of eddy current probes (ECP) based on single or multiple giant magneto-resistance (GMR) sensors [4]. The use of GMRs is a good tested choice for the present application.
When a GMR is used, the obtained images represent one component of the magnetic induction field along the sensing axis. With these images it is possible to detect the presence of flaws. The estimation of the geometrical characteristics of the flaws is carried out using the amplitude and the phase evolution profile for a tested area [5]. Normalization, filtering, image segmentation, feature extraction and classification techniques [6] are used to evaluate the specific characteristics of those detected flaws.
This paper continues previous works on non-destructive testing of aluminum plates [7,8]. However, a particular case of flaw detection in an aluminum plate welded zone is considered. New elements concerning the specific eddy current test (ECT) probe architectures including coils and GMR sensors are an important part of this work. Referring to the image processing that is particularly associated with the flaw detection in the welded zone, a practical approach on optimal image filtering for a better detection of the flaws is included in the work.

2. EXPERIMENTAL METHODS

The welded zone testing is performed using a non-destructive test (NDT) system setup that includes an eddy current testing probe attached to a XY scanning stage working under a PXI system. The PXI system includes several modules associated with the generation of the excitation signal, the acquisition of the ECP output and the control of a Kuroda-XY scanning stage. Additionally, several circuits such as a power trans-admittance amplifier based on a TPA02 operational amplifier, and a low noise amplifier based on the INA118 instrumentation amplifier are part of the testing system.
The signals from the conditioning circuits associated with the sensing probes are applied to one analog input of the data acquisition module and the digital values of the acquired voltages are processed on a PC computer in order to obtain the images that express the amplitude and the phase variation of the detected signals for a scanned welded zone of the aluminum plate. The phase measurement is obtained acquiring the excitation current that flows through a sampling resistor in another channel of the data acquisition module within the PXI system. The obtained images are analyzed off-line for flaw detection on the welded zone.

ISBN 978-963-88410-0-1

2.1. Eddy current testing probe (ECT-probe)

Two architectures of eddy current testing probes are considered in the work: one classical inductive probe (ECT-IP) with three coaxial coils, one for excitation and two detection coils as depicted in Fig.1.a, and a probe (ECT-PP) with one excitation coil and a GMR sensor with the sensing plane perpendicular to the coil axis as depicted in Fig. 1.b.

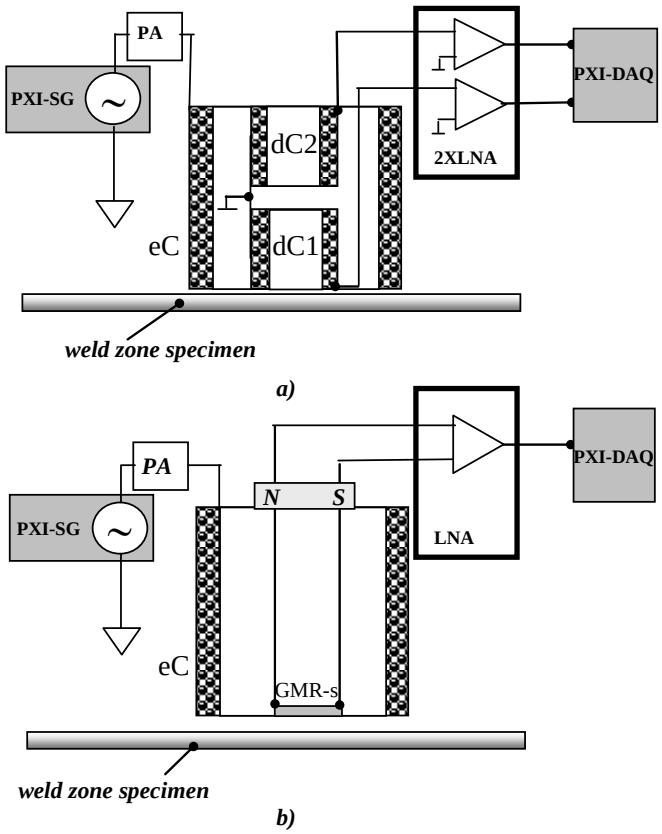

Fig.1. ECT probes a) ECT-IP probe; b) ECT-PP probe; eC - excitation coil; dC1, dC2 - detection coils; GMR – giant magneto-resistive sensor; LNA-low noise amplifier, PA-power trans-admittance amplifier, PXI-SG -modular signal generator, PXI-DAQ -acquisition module.

The excitation coils (eC) of the ECT probes are characterized by the following parameters: inside radius 20 mm, outside radius 46 mm, length of coil 10 mm, number of turns 400, diameter of wire 0.5 mm. The detection coils of the 1eC-2dC ECT probe present the following characteristics: inside radius 2 mm, outside radius 3 mm, length of coil 5 mm, number of turns 500, diameter of wire 0.1 mm. Referring to 1eC-1GMR ECT probe the induction field is measured using the GMR (NVE-AA002) sensor with the geometric characteristics according to the SOIC-8 standard values. The used GMR presents the detection direction normal to the excitation coil symmetry axis and presents a linear operation range between 1.5 Oe to 10.5 Oe and sensitivity in the range between 3.0 mV/V-Oe and 4.2 mV/V-Oe. A permanent magnet is used to assure the GMR biasing, providing a constant magnetic field in the sensitive direction.

2.2. Signal Conditioning

The excitation current is produced by a trans-admittance amplifier driven by a NI PXI-5406 function generator. The voltage signals obtained from the eddy current probes: V_{dC1} and V_{dC2} in the inductive probe case and V_{GMR} in the ECT probe based on GMR are amplified on the low noise amplifier stage that was implemented using an INA118. Different gain values are automatically set (G_{ind} = 100, 150, 200).

The detected signals are applied to the analog inputs of the PXI-6251 16-bit multifunction board working with a maximum acquisition rate of 1.2 MHz.

For each position of both ECT probes the output signals are acquired during some periods of the excitation current. The estimation of the signal amplitude, phase and frequency is obtained using the LabVIEW "tone measurement function".

For the particular case of the inductive ECT-IP probe, the signal V_{IP} that contains the information on the defects is obtained by subtracting the estimated phasors derived from the detection coils voltages. For the ECT-PP probe a V_{MP} signal, containing the information on the defects, is obtained directly from the tone measurement function output for the V_{MS}.

The calculated V_{IP} or V_{MP} are stored together with the (x,y) coordinates of the corresponding probe localization on the plate. Thus an EC image is obtained and will be analyzed for cracks and flaw detection and characterization.

In order to provide the excitation current to the probes, at different frequencies, a PXI generator and a power amplifier (PA) is used. The ECT-probes are excited by a sinusoidal current with frequency within the [2; 15] kHz range for 1eC-2dC ECT probe and [0.1; 10] kHz for the 1eC-1GMR ECT probe. Varying the frequency a good sensitivity for the detection of superficial defects or deeper field penetration into the tested aluminum plates is reached. The sensitivity of the magneto-resistive sensor included in the probe does not depend on the frequency in the considered range. Thus, the overall probe sensitivity is increased in what concerns the detection of flaws deeper in the welded region.

3. IMAGE SIGNAL PROCESSING

The signals acquired from the detectors for the sinusoidal excitation are processed in order to obtain the eddy current amplitude images (EC-AI) and eddy current phase images (EC-PI). The pixel dimension depends on the X-Y scanning stage resolution. However, to limit the total amount of data, 0.5 mm × 0.5 mm and 1 mm × 1mm per pixel were considered in the present case.

The eddy current images were obtained for an aluminum welded plate where the weld defects have been purposely created. These defects consist of incomplete weld, weld with impurities, and lack of weld.

In order to detect the induced defects in the welded zone the acquired images were processed in different steps. Normalization followed by RGB to gray 8-bit image conversion, image filtering using stationary wavelet methods, image segmentation and the estimation of the geometric characteristics of the defects in the resulting binary image.

3.1. ECI normalization

For an eddy current image (ECI) of the welded zone (e.g. 60×40 mm specimen) the pixels intensity (ECI(x,y)) were represented as integer values using the relation:

$$ECI(x,y) = 2^N \times \text{round}\left(\frac{v_p(x,y) - \min v_p}{\max v_p - \min v_p}\right) \qquad (1)$$

where $\boldsymbol{v_p}$ represents the matrix of the acquired signal amplitudes or phase differences, considering the excitation current as reference, and N is the image resolution.

For a low computational load and considering that the Matlab image processing functions are usually tailored for unsigned 8-bit images, the present work refers to $N = 8$.

3.2. ECI filtering

The eddy current images (ECI) previously obtained were analyzed into the wavelet domain by using the 2D stationary wavelet transform (2D-SWT) followed by a soft thresholding technique in order to preserve the localization of the defects on the welded zone. The processed image was reconstructed using the 2D stationary inverse wavelet transform (2D-ISWT).

The 2D-SWT was used because of its ability to perform the accurate local analysis of an arbitrary image and to assure the positional integrity that is an urged condition in the present case. Using the presented filtering, based on 2D-SWT, the segmentation is well performed even when the background pixel intensity levels are not uniform due to the welding line.

The ECI filtering was required considering that during eddy current sensing, using the inductive or the magneto-resistive based probe, the XY controlled motion system and the sensors geometry is associated with the linear motion and with unfocussed effects at the ECI level.

For the decompositions based on 2D-SWT, the data are simply decomposed into a high frequency component (H) and a low-frequency component (L). Therefore, in the 1st level of decomposition, the input image is divided into HH, HL, LH, and LL components, where high-frequency is considered in the row direction and low-frequency in the column direction as HL and so on. The same decomposition is continued recursively for the LL component.

As is presented in Fig.2, after the 1st level decomposition based on 2D-SWT, the coefficient details corresponding to horizontal, vertical or diagonal directions (HH, LL, LH and HL) are applied to the input of the soft thresholding processing block.

The general soft-threshold function is defined by:

$$\beta_T(x) = \text{sign}(x) \times \max(|x| - T, 0) \qquad (2)$$

This function takes the argument and shrinks it toward zero using the threshold T [9-10]. It was particularly adapted for the 2D-SWT details thresholding. Using this procedure the noise is removed discriminating the wavelet coefficients by sub-bands, but keeping the low resolution coefficients unaltered.

The processed 2D-SWT details and the LL (SWT 1st level approximation) are used to reconstruct the filtered eddy current image ECI_{swf}, using the inverse 2D stationary wavelet transform.

3.3. ECI segmentation

The filtered images were applied to the segmentation and ECI_{swf} feature detection and measurement processing block.

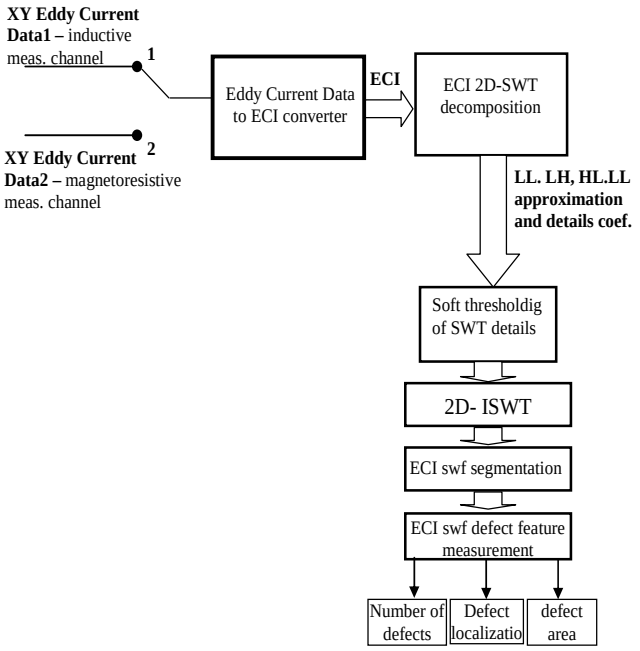

Fig.2. ECI processing block diagram (ECI-eddy current image; LL, LH, HL, LL -1st level 2D-SWT decomposition approximation and details)

In the segmentation process a global threshold level was used to convert the ECI_{swf} intensity image into a corresponding binary image ECI_B.

The Matlab functions used for ECI_{swf} segmentation were "graythresh(.)" and "im2bw(.)". Accordingly, measurement accuracy results and additional techniques based on 2D-SWT direct segmentation were also considered.

The image elements obtained were the number of defects in the welded zone, their localization, and the area of each one. These elements were estimated starting from the ECI_B.

Considering the scanned region and the number of pixels for the considered ECI the localization and the crack area were estimated. The localization of the image features was obtained by estimation of the centroid position in the ECI_B, while the areas were calculated as the sum of the pixels for each image object multiplied by the area of the individual pixels. In order to characterize the accuracy of the implemented ECI processing, a comparison between the real localization and pixel size with the obtained results was considered because the plate sample had been previously characterized..

4. RESULTS AND DISCUSSION

Two sets of eddy current images were obtained using both types of ECT probes. For the particular case of ECT prove based on GMR for a 10X40 mm scanned area the evolution

of amplitude (ampl) and phase (ph) are presented in Fig.3 and Fig.4. These results were obtained with an excitation frequency $f_{ex} = 7$ kHz . For this excitation frequency the standard penetration depth in the Al 2024 T3 aluminum is $\delta = 4,55$ mm . The sampling frequency is set automatically being dependent on the number of points per period introduced in the LabVIEW application. In the present case the sample frequency was $f_S = 210$ kHz corresponding to 30 points per period at $f_{ex} = 7$ kHz . In order to get a good accuracy on the amplitude and phase calculation, based on the tone measurement LabVIEW function, 20 periods were acquired, with a total of 600 samples for each position of the probe. One measurement is taken for each position of the probe, but the time required to accomplish the measurement depends essentially on the required delay to stabilize the mechanical system (e.g. 3 sec.). The image processing if performed offline only after the entire surface was scanned.

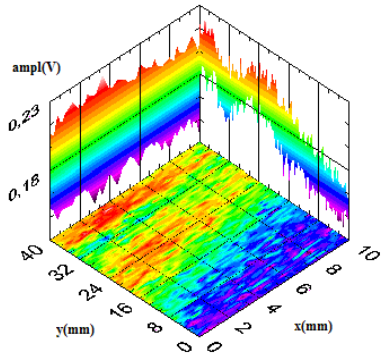

Fig.3. The evolution of the eddy current amplitude for a 10X40 mm welded zone.

When the ECT-PP probe, based on a GMR sensor, is used the localization of the weld line is clearer when the phase difference profile is observed than by inspecting the amplitude profile.

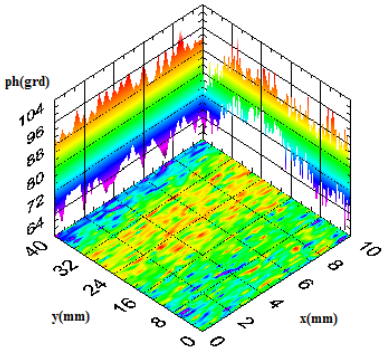

Fig.4. The evolution of the phase difference between the excitation current and eddy currents for a 10X40 mm welded zone.

Using the ECT-IP probe based on excitation and detection coils the amplitude evolution corresponding to the welded zone assures a better localization of the weld line.
After normalization an 8-bit gray image of the weld zone is obtained. Fig. 5 presents the 8-bit gray image (124x84 pixels, 1 pixel occupying a 0.5×0.5 mm square) obtained using the ECT-IP probe for the weld scanned region. The dark gray vertical bar is due to the morphological material change in the weld line, but a defect is visible on the upper top of this line.

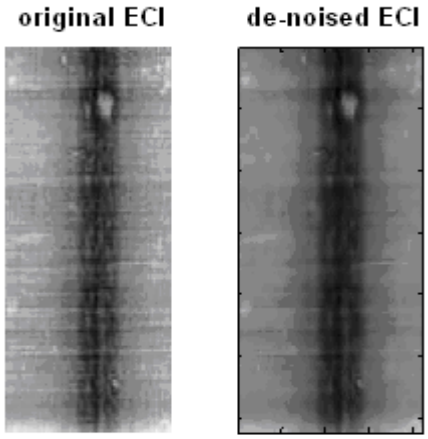

Fig.5. Normalized 8-bit eddy current image before and after 2D-SWT filtering.

After filtering the segmentation based on the thresholding method was applied and a binary image was obtained (Fig.6). An additional processing, using the bwareaopen (.) function, was applied to remove the objects containing a small number of pixels (N<4 pixels) from the binary image represented in Fig.6 a). To fill the gaps the strell(.) Matlab function was used and the Fig. 6 b) was obtained. The parameters used on the applied functions were chosen in order not to affect the main geometrical characteristics of the detected defect represented on the binary image.

a) b)

Fig.6 The binary image obtained after segmentation of the de-noised ECI gray image.

Using the binary image feature extraction based on the *imfeature(.)* Matlab function, the defect position on the scanned area was determined based on centroid estimation. For the particular case of Fig.6 the centroid coordinates are x_c=19 pixels, y_c=51 pixels. The area of the detected defect was calculated also in pixels and is about 32 pixels. Taking into account the scanning step of 0.5 mm the area of the defect in the weld zone is about 8 mm^2.

5. CONCLUSIONS

In this paper a practical approach concerning eddy current non destructive testing with image processing, using two types of eddy current probes, one based on excitation and detection coils and another based on an excitation coil and a GMR sensor, was presented. Image filtering techniques based on a 2D stationary wavelet transform are used to diminish the noise influence on the weld defects. After ECI filtering, the segmentation and feature extraction was applied in order to extract the geometrical characteristics of the detected defects. The implemented software for the off-line image processing proved to be a good solution in what concerns the defect localization and to estimate the defect area in the weld region. The geometrical measurements of the induced defects in the welded zone were done using images that were obtained for both probes associated with the developed automated measurement system for NDT testing.

As future work, the increasing of the ECI image quality, with the inclusion of the liftoff correction and the possibility of performing on-line detection will be addressed.

ACKNOWLEDGMENT

This work was developed under the project PTDC/EEA-ELC/67719/2006 supported in part by the Portuguese Science and Technology Foundation (FCT). This support is gratefully acknowledged.

REFERENCES

[1] A. Bernieri, L. Ferrigno, M. Laracca, M. Molinara, "Crack Shape Reconstruction in Eddy Current Testing Using Machine Learning Systems for Regression", IEEE Transactions on Instrumentation and Measurement, Vol. 57, N.9, pp. 1958-1968, Sept. 2008.

[2] H.Hoshikawa and K.Koyama : "Eddy Current Testing by Uniform Eddy Current Probe" , Proceedings of 4th Far East Conference on NDT , pp43-52 (1997).

[3] O. Postolache, M.D. Pereira, H. Ramos, A. Ribeiro, "NDT on Aluminum Aircraft Plates based on Eddy Current Sensing and Image Processing", Proc IEEE International Instrumentation and Technology Conf, I2MTC, Victoria, Vol I, pp 1803-1808, 2008.

[4] T. Dogaru, "Giant Magnetoresitance based Eddy-Current Sensor", IEEE Transactions on Magnetics, Vol. 37, No. 5, pp.3831-3838, 2001.

[5] J. Pavo, K. Miya, "Optimal design of eddy current testing probe using fluxset magnetic field sensors", IEEE Transactions on Magnetics, Vol 32, pp. 1597-1600, May. 1996.

[6] R. Woods, D.J. Czitrom, S. Armitage, R.C. Gonzalez, *Digital Image Processing*, Prentice Hall, 2007.

[7] H.G. Ramos, A.L. Ribeiro, P. Ježdík, J. Neškudla, M. Kubinyi,"Eddy Current Testing of Conducting Materials", Proc IEEE International Instrumentation and Technology Conf, I2MTC, Victoria, pp. 964-968, 2008.

[8] O. Postolache, H.G. Ramos, A. L. Ribeiro, "Characterization of Defects in Aluminum Plates Using GMR Probes and Neural Network Signal Processing", Proc.16th IMEKO TC4 Symposium, Florence-Italy, Sept. 2008.

[9] Choi Hyeokho, R. Baraniuk, "Analysis of wavelet-domain Wiener filters", Proceedings of the IEEE-SP International Symposium on Time-Frequency and Time-Scale Analysis, pp. 613-616 , Oct. 1998.

[10] F. Jin, P. Fieguth, L. Winger, E. Jernigan, "Adaptive Wiener filtering of noisy images and image sequences", International Conference on Image Processing, Vol. 3, Sep. 2003.